

Kinetic study of decomposition for Co(II)- and Ni(II)-1,10-phenanthroline complexes intercalated in γ -zirconium phosphate

Stefano Vecchio · Romolo Di Rocco ·
Carla Ferragina

AICAT2008 Conference
© Akadémiai Kiadó, Budapest, Hungary 2009

Abstract The thermal behaviour of the complexes formed in situ between the aromatic diamine 1,10-phenanthroline and the Co(II) and Ni(II) ions intercalated between the layers of γ -zirconium phosphate was studied by simultaneous TG/DSC techniques. The obtained materials show similar thermal behaviour: after a multi-step dehydration process they showed an oxidative decomposition in only one step. The kinetic study of the decomposition process was performed using both the model-free methods of Ozawa-Flynn-Wall and Kissinger. The former method provides a negligible dependence of activation energy on the degree of reaction α for both materials. Activation energies derived by the Kissinger method show a good agreement with the mean values derived by the Ozawa-Flynn-Wall method. The Arrhenius rate constants determined using also the pre-exponential factor values demonstrate that their thermal stability can be considered comparable, within the experimental uncertainty. Finally, a reliable method was applied to determine the model function from the best fit between the numerical dependence of the integral function $g(\alpha)$ vs. α and several theoretical model dependencies reported in literature for the most commonly used models. A Mampel first-order reaction model was selected to describe the thermal decomposition in both the materials studied.

Keywords Ion-exchanger · Layered materials · Simultaneous TG/DSC · Decomposition kinetics · Kissinger method · Ozawa-Flynn-Wall method

Introduction

Acid phosphates of tetravalent metals of general formula $\text{Me(IV)}(\text{PO}_4)_2 \cdot n\text{H}_2\text{O}$ ($\text{Me} = \text{Zr, Ti, Sn...}; n = 1, 2...$) are insoluble ion-exchangers that can be prepared in crystalline forms with non rigid layered structures. These materials are well known to exchange metal ions [1, 2], to intercalate organic bases [3] and to support non polar molecules [4, 5]. In our previous papers intercalation compounds were obtained by intercalating aromatic diamines such as 2,2'-bipyridyl, 1,10-phenanthroline and 2,9-dimethyl-1,10-phenanthroline between the layers of α -zirconium phosphate and γ -zirconium or titanium phosphate, giving well ordered organic-inorganic compounds. Transition metal ions such as Co(II), Ni(II) and Cu(II) inserted into such compounds by ion-exchange can be subsequently coordinated to the bases throughout the layers giving rise to complexes in situ formed [6–9]. These materials were prepared with the aim to obtain either catalysts or catalyst precursors suitable to be used in heterogeneous catalysis by complexes usually utilized in the homogeneous catalysis [10–12]. As a continuation of previous studies [13–15] in the present investigation γ -zirconium phosphate [γ -Zr(PO_4)(H_2PO_4) $\cdot 2\text{H}_2\text{O}$, γ -ZrP] was intercalated with 1,10-phenanthroline (phen) and denoted as γ -ZrPphen and subsequently exchanged with Co(II) and Ni(II) ions to give complex formed in situ (γ -ZrPphenCo, γ -ZrPphenNi). This study is devoted to characterize the thermal oxidative decomposition of these two intercalation materials using two different kinetic methods and provide reliable Arrhenius parameters and a

S. Vecchio (✉)
Dipartimento di Ingegneria Chimica Materiali Ambiente,
Sapienza Università di Roma, Via del Castro Laurenziano 7,
00161 Rome, Italy
e-mail: stefano.vecchio@uniroma1.it

R. Di Rocco · C. Ferragina
Istituto di Metodologie Inorganiche e dei Plasmi, CNR,
Via Salaria km. 29.300, 00016 Monterotondo, Rome, Italy

suitable model function for the process studied in each material. On the other hand, to the best of our knowledge, no relevant information are available in literature on the oxidative decomposition kinetics of phen when it is intercalated (as such or as a complex with a divalent metal ion) between the layers of these ion-exchangers except for the studies published by our group [13–15].

Experimental and method

Chemicals and materials

The cobalt acetate, nickel acetate, zirconyl chloride, phosphoric acid and 1,10-phenanthroline were supplied by Aldrich (reagent grade) and used without further purification. The precursors γ -ZrP and the intercalation compound γ -ZrPphen were prepared as reported in literature ([16] and [9], respectively), while the syntheses of both γ -ZrPphenCo and γ -ZrPphenNi were carried out according to the same procedure adopted for the analogue γ -ZrPphenCu reported in a previous paper [13].

Physical measurements and chemical analysis

Cobalt and nickel ions were determined in the supernatant solutions, before and after contact with the exchanger with a GBC 903 A.A. spectrophotometer. Phosphates were determined colorimetrically [17]. X-ray powder diffraction (XRPD) was used to study phase changes in the materials by monitoring the reflection and its harmonics. A Philips diffractometer (model PW 1130/00) was used with Ni-filtered Cu K_α radiation ($\lambda = 1.541 \text{ \AA}$).

Thermal measurements

The TG and DSC experimental measurements were carried out on a simultaneous Stanton Redcroft 625 thermoanalyzer, connected to 386 IBM-compatible personal computer. Thermodynamic quantities were calculated using the Stanton-Redcroft Data Acquisition System, Trace 2, Version 4. Temperature and heat flow rate scales were calibrated with very pure standards (indium, lead, tin, zinc), whose melting temperatures and enthalpies are well known [18]. Samples of 6–8 mg were weighed into Al pans in an argon-filled dry box to avoid a possible sample degradation, and then in the thermoanalyzer, where the purge air stream fluxed to continuously remove the gases given off during the thermal heating process experiment. Three TG/DSC experiments were made for each material at 8 K min^{-1} using fresh samples only and a good precision of experimental data was obtained (<1%). On the other hand, for the kinetic analysis the TG/DSC measurements

have been carried out at different heating rates (2, 4, 6 and 8 K min^{-1}) up to 873 K under a 100 mL min^{-1} stream of air.

Kinetic procedure and selection of the most suitable reaction mechanism

The kinetics of solid state decompositions applied in this study is usually described by a sequence of basic equations and statements whose details are reported in our previous papers [13–15]. In particular, the first kinetic method used was the isoconversional method of Ozawa-Flynn-Wall (OFW) [19, 20] according to the following isoconversional equations

$$\ln(\beta)_\alpha = \ln[(A_\alpha E_\alpha)/R] - \ln g(\alpha) - 5.3305 - 1.052(E_\alpha/R)(1/T_\alpha) \quad (1)$$

where $g(\alpha) = \int_0^\alpha f(\alpha)^{-1} d\alpha$ is the integral form of the model function⁰ that does not depend on the heating rate used, whose mathematical expressions are reported in Table 1 [21]. Once the Doyle's approximation [22]: $\ln p(x) \approx -5.3305 - 1.052x$, where $x = E_\alpha/(RT_\alpha)$ and $20 \leq x \leq 60$ is verified to be valid over the entire range of α , then at any selected value of α , from the slope of the related regression straight line derived by the $\ln(\beta)$ vs. $1/T_\alpha$ plot, the corresponding E_α value is derived as a function of α . The present kinetic study was also performed using the Kissinger method [23] that uses the following equation:

$$\ln(\beta/T_m^2) = \ln[(AR)/E] + (-E/R)(1/T_m) \quad (2)$$

where T_m is the DSC peak temperature at a given heating rate β . From the slope of Eq. 2 a single activation energy value for each step of mass loss is given.

Subsequently, TG data derived by a single linear heating rate experiment were fitted to some of the integral model functions $g(\alpha)$ reported in literature [24] (Table 1) using the Coats-Redfern (CR) method [25]. This method makes the assumption that the integral model function

$$\ln[g_j(\alpha)/T^2] = \ln\{[(A_j R)/(\beta E)] [1 - (2R \langle T \rangle / E_j)] - E_j / (RT)\} \quad (3)$$

where the subscript j is related to the selected reaction model and $\langle T \rangle$ is the average of the experimental temperature range. Each $g_j(\alpha)$ expression in Table 1 is inserted in Eq. 3 and from the slope of the linear regression obtained by plotting $\ln[g_j(\alpha)/T^2]$ against $1/T$ the corresponding Arrhenius parameters E_j and A_j are obtained for each model function j . These Arrhenius parameters related to all the different model function j of the same process are linearly correlated (compensation effect). The linear regression parameters obtained were used to estimate the isoconversional $\ln A_\alpha$ value at each given conversion by replacing the E_j values

Table 1 Most commonly used differential and integral model functions to describe the thermal decomposition processes

N	Model function	$f(\alpha)$	$g(\alpha) = kt$
1	Power law	$4(\alpha)^{3/4}$	$(\alpha)^{1/4}$
2	Power law	$3(\alpha)^{2/3}$	$(\alpha)^{1/3}$
3	Power law	$2(\alpha)^{1/2}$	$(\alpha)^{1/2}$
4	Power law	$(2/3)(\alpha)^{-1/2}$	$(\alpha)^{3/2}$
5	One-dimensional diffusion	$1/(2\alpha)$	$(\alpha)^2$
6	Mampel (first-order)	$1 - \alpha$	$-\ln(1 - \alpha)$
7	Avrami-Erofeev	$4(1 - \alpha)[- \ln(1 - \alpha)]^{3/4}$	$[- \ln(1 - \alpha)]^{1/4}$
8	Avrami-Erofeev	$3(1 - \alpha)[- \ln(1 - \alpha)]^{2/3}$	$[- \ln(1 - \alpha)]^{1/3}$
9	Avrami-Erofeev	$2(1 - \alpha)[- \ln(1 - \alpha)]^{1/2}$	$[- \ln(1 - \alpha)]^{1/2}$
10	Three-dimensional diffusion	$(3/2)(1 - \alpha)^{2/3}[1 - (1 - \alpha)^{1/3}]^{-1}$	$[1 - (1 - \alpha)^{1/3}]^2$
11	Contracting sphere	$3(1 - \alpha)^{2/3}$	$1 - (1 - \alpha)^{1/3}$
12	Contracting cylinder	$2(1 - \alpha)^{1/2}$	$1 - (1 - \alpha)^{1/2}$
13	Zero-order	1	α
14	Second-order	$(1 - \alpha)^2$	$(1 - \alpha)^{-1} - 1$

with the isoconversional E_x ones in the regression equation [26]. The integrated model function $g(\alpha)$ can be numerically reconstructed using an artificial isokinetic relationship [26, 27] if the values of E_x are practically independent of α . Once the values of $\ln A_x$ and E_x are determined the integrated model function $g(\alpha)$ is reconstructed by substituting the selected estimates of A_x and E_x in the following equation:

$$g(\alpha) = (A/\beta) \int_0^T \exp(-E/RT) dT. \quad (4)$$

The explicit form of the model function can be determined by comparing the selected numerical dependence of $g(\alpha)$ vs. α with the 14 different model dependencies displayed in Table 1 searching for the model having the best match with the numerical dependence obtained by processing experimental data.

Results and discussion

Chemical and structural characterizations

The water and phen contents were determined by the mass losses recorded by the corresponding TG curves in their characteristic temperature ranges. The chemical formulas proposed on the basis of chemical and thermal analysis are: $\gamma\text{-Zr}(\text{PO}_4)(\text{H}_2\text{PO}_4)\text{phen}_{0.50} \cdot 3\text{H}_2\text{O}$; $\gamma\text{-Zr}(\text{PO}_4)(\text{HPO}_4)\text{phen}_{0.50} \text{Co}_{0.50} \cdot 2.20\text{H}_2\text{O}$ and $\gamma\text{-Zr}(\text{PO}_4)(\text{HPO}_4)\text{phen}_{0.50} \text{Ni}_{0.50} \cdot 1.90 \text{H}_2\text{O}$. From the XRPD patterns of $\gamma\text{-ZrPphen}$; $\gamma\text{-ZrPphenCo}$ and $\gamma\text{-ZrPphenNi}$ at room temperature their interlayer distance d are 18.50, 16.71 and 17.26 Å, respectively. As a consequence of the intercalation process an expansion of the d value was observed in the case of the precursor $\gamma\text{-ZrP}$ in

comparison with $\gamma\text{-ZrPphen}$ (12.30 Å vs. 18.50 Å respectively). It is worth noting that the complex formation not always occurs with an increase of d .

Thermal behaviour and kinetic analysis

The TG, DTG and DSC curves of ZrPphenCo and $\gamma\text{-ZrPphenNi}$ are given in Figs. 1 and 2. The thermal behaviour is quite similar to that of $\gamma\text{-ZrPphenCu}$,

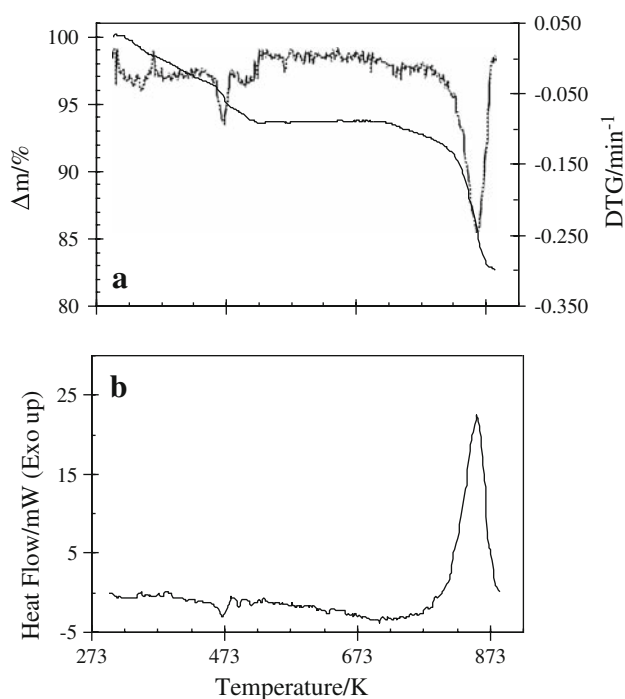


Fig. 1 Thermoanalytical curves of $\gamma\text{-ZrPphenCo}$ at 6 K min^{-1} : **a** TG and DTG curves (solid and thin lines, respectively) and **b** DSC curve

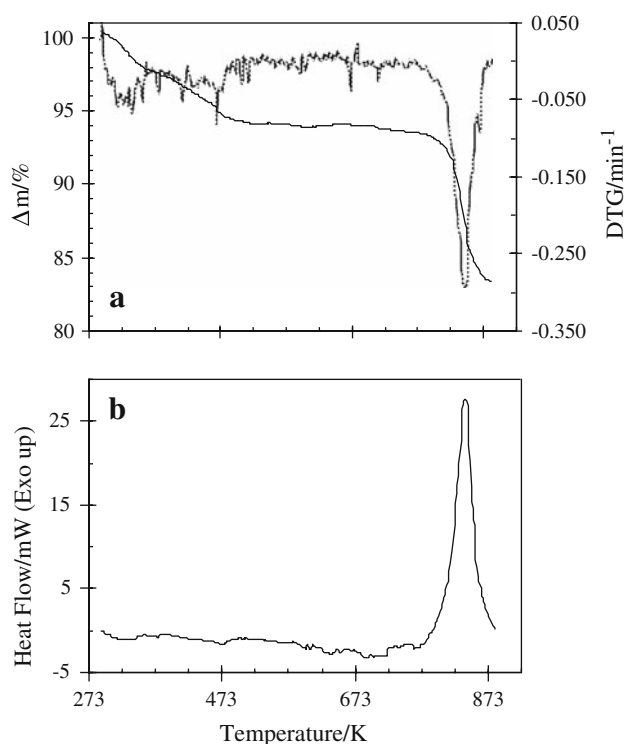


Fig. 2 Thermoanalytical curves of γ -ZrPphenNi at 6 K min^{-1} : **a** TG and DTG curves (solid and thin lines, respectively) and **b** DSC curve

published in a previous paper [13]. In fact, in the two intercalation Co and Ni materials examined a single noticeable exothermic effect ascribed to decomposition of phen occurs with a simultaneous single step of mass loss

Fig. 3 Dependency of the activation energy on α (OFW method) for the decomposition process in: **a** γ -ZrPphenCo and **b** γ -ZrPphenNi

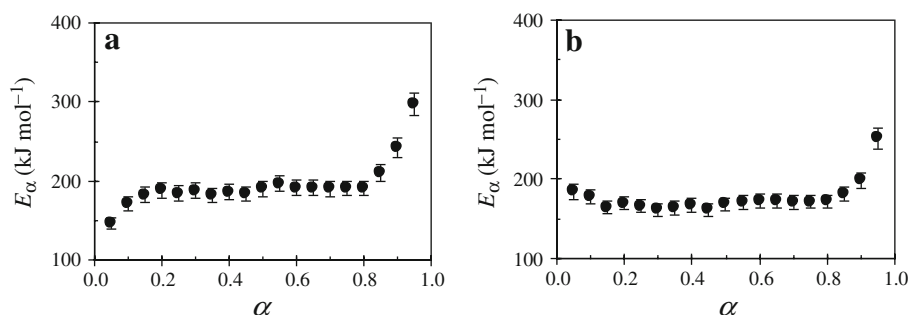


Table 2 Kinetic parameters for the thermal decomposition step of the materials examined using the Kissinger method

Materials	Arrhenius parameters		R^{2a}	$\langle T \rangle / \text{K}$	$\ln k / \text{min}^{-1} \text{ } ^b$	Reference
	$E / \text{kJ mol}^{-1}$	$\ln A / \text{min}^{-1}$				
γ -ZrPphenCo	193 ± 6	26 ± 1	0.9977	845.8	-1.9	This work
γ -ZrPphenNi	162 ± 7	21 ± 1	0.9950	829.4	-2.1	This work
γ -ZrPphenCu	180 ± 4	24 ± 1	0.9961	749.5	-5.1	[13]

The associated uncertainty are standard deviations

^a R = Square of the correlation coefficient for n data points ($n = 4$)

^b Calculated at $T = \langle T \rangle$

(9.7% and 12.6% for γ -ZrPphenCo and γ -ZrPphenNi, respectively) from 673 to 873 K after more or less evident dehydration processes. The mean values of the DSC peak temperatures associated to the decomposition step are comparable for the two materials and significantly higher than that observed for the intercalation Cu material in a previous paper [13].

As far as the results of the kinetic study of the oxidative decomposition process is concerned, the OFW method showed E_α values practically constant over a wide range of α (within the experimental errors estimated) with an evident increasing trend in limited ranges: $\alpha \leq 0.1$ (only for γ -ZrPphenCo) and $\alpha > 0.70$ (for both materials) (Fig. 3a, b). Contrary to what it could be expected taking into account the usual complex nature of thermal decomposition processes, but similarly to what was found recently for γ -ZrP and γ -TiP intercalation materials containing the 1:1 complex between 2,2'-bipyridyl and Cu [15], the main part of the reaction has a single-step nature describable by a single reaction mechanism. Therefore, the Kissinger method can be considered suitable to analyze these processes. The Arrhenius parameters, the mean values of the experimental temperature range $\langle T \rangle$ and the $\ln k$ values calculated at $T = \langle T \rangle$ were summarized in Table 2 for both materials investigated and were recalculated for γ -ZrPphenCu using the results reported in literature [13], for comparison purposes. The $\ln k$ values related to the decomposition processes of Co(II) and Ni(II) intercalation materials are not significantly different (even if the Arrhenius parameters of the former are slightly higher than those of the latter).

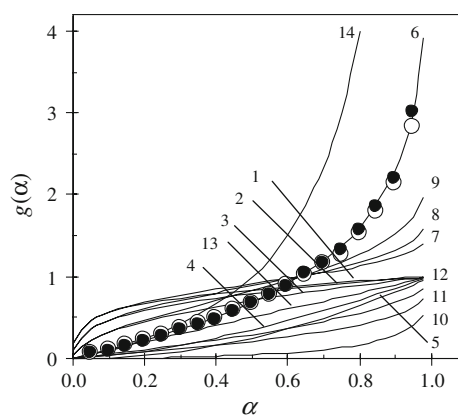


Fig. 4 Conversion dependence of $g(\alpha)$ for the model functions listed in Table 1 (—) and for the experimental data related to decomposition of: γ -ZrPphenCo (open circle), γ -ZrPphenNi (filled circle)

Remarkable lower rate constant value (and lower thermal stability) was determined for the decomposition of the Cu(II) intercalation material studied previously [13], even if no relevant differences in the Arrhenius parameters were observed with the Co(II) and Cu(II) materials. The average E values determined using the OFW method agree quite well with those of the Kissinger one within the associated experimental errors. In addition, the negligible dependence of E on the degree of conversion α for the oxidative decomposition process of the two intercalated materials examined in the range $\alpha \leq 0.7$, enable the most suitable model functions to be selected using the procedure reported in the Experimental section of this paper. To this end, the comparison of the numerical dependence of $g(\alpha)$ vs. α determined by processing kinetic data and the theoretical dependence related to all the 12 models listed in Table 1 is given in Fig. 4. A good agreement with the first-order Mampel model (model no. 6 in Table 1) [28] is found for the oxidative decomposition of both intercalation materials over the entire range of α .

Conclusions

As a result of the present study, thermal analysis (in particular TG and DSC), coupled with XRPD are very useful techniques to carry out an exhaustive structural characterization of layered inorganic materials like those presented in this paper and to assess a thermal stability scale related to an homologues series of materials. In particular, it was confirmed that both the intercalation materials examined presented similar thermal behaviour, but different with respect to the analogue γ -ZrPphenCu. Identical decomposition mechanisms and, on the basis of the rate constant values, comparable thermal stabilities are also obtained.

Acknowledgements The authors greatly acknowledge the Italian C.N.R. and M.I.U.R. for their financial supports.

References

1. Clearfield A, Kalnins JM. On the mechanism of ion exchange in zirconium phosphates-XIII. *J Inorg Nucl Chem.* 1976;38:849–52.
2. Clearfield A. Effect of crystallinity on the ion-exchange of metal ions in zirconium phosphates. In: Clearfield A, editor. *Inorganic ion-exchange materials.* Boca Raton, FL: CRC Press; 1982. p. 20–7.
3. Ferragina C, Massucci MA, La Ginestra A, Patrono P. Pillaring of layers in α -zirconium phosphate by 1,10-phenanthroline and bis (1,10-phenanthroline) copper(II). *J Chem Soc Dalton Trans.* 1986:2265–71.
4. Ferragina C, Cafarelli P, Di Rocco R. Incorporation of cadmium ions and cadmium sulfide particles into sol-gel zirconium phosphate. *J Therm Anal Calorim.* 2001;63:709–21.
5. Ferragina C, Di Rocco R, Petrilli L. Zinc ions and zinc sulfide particles in sol-gel zirconium phosphate synthesis, thermal behaviour and X-ray characterization. *Thermochim Acta.* 2004;409:177–87.
6. Ferragina C, Massucci MA, Patrono P, Tomlinson AAG, La Ginestra A. Pillars chemistry. Part 4. Palladium (II)-2,2'-bipyridyl-1,10-phenanthroline, and -2,9-dimethyl-1,10-phenanthroline complex pillars in α -zirconium phosphate. *J Chem Soc Dalton Trans.* 1988:851–7.
7. Ferragina C, La Ginestra A, Massucci MA, Cafarelli P, Di Rocco R. Thermal behaviour of copper-dimethyl-phenanthroline species in α - and γ -zirconium phosphates. *J Therm Anal.* 1994;41:1469–78.
8. Ferragina C, Cafarelli P. γ -zirconium and γ -titanium phosphates platinum intercalation compound. *J Therm Anal.* 1998;53:189–206.
9. Ferragina C, Massucci MA, Tomlinson AAG. Pillar chemistry. Part 5. Intercalation of 2,2'-bipyridine, 1,10-phenanthroline and 2,9-dimethyl-1,10-phenanthroline into γ -zirconium phosphate and formation of interlayer copper(II) complexes. *J Chem Soc Dalton Trans.* 1990:1191–6.
10. Ferragina C, La Ginestra A, Massucci MA, Patrono P, Giannoccaro P, Nobile F, et al. Oxidative carbonylation of aniline catalyzed by Pd(II)-2,2'-bipyridyl complex intercalated in α -zirconium phosphate. *J Mol Catal.* 1989;53:349–57.
11. Lenarda M, Ganzerla RL, Zanoni R. Catalysis by the Rh/B system. Part 1. Vapour-phase hydroformylation of ethylene at atmospheric pressure on Rh/B on silica. *J Mol Catal.* 1993;78:339–50.
12. Giannoccaro P, Doronzo S, Ferragina C. Rh^{3+} ions and Rh^{3+} -diamine complexes intercalated in α - and γ -zirconium phosphate as stable and effective catalysts for the conversion of aniline or nitrobenzene to carbamates and/or N,N'-diphenylurea. Part 3. In: Blaser HU, Baiker A, Prins R, editors. *Heterogeneous catalysis and fine chemicals*, vol. IV. New York: Elsevier Science; 1997. p. 633–40.
13. Vecchio S, Di Rocco R, Ferragina C, Materazzi S. Thermal and kinetic study of dehydration and decomposition processes for copper intercalated γ -zirconium and γ -titanium phosphates. *Thermochim Acta.* 2005;435:181–7.
14. Vecchio S, Di Rocco R, Ferragina C. Intercalation compounds of γ -zirconium and γ -titanium phosphates. Kinetic study of dehydration and decomposition processes for 2,9-dimethyl-1,10-phenanthroline and its intercalated copper complex materials. *Thermochim Acta.* 2007;453:105–14.
15. Vecchio S, Di Rocco R, Ferragina C. Kinetic analysis of the oxidative decomposition in γ -zirconium and γ -titanium phosphate

- intercalation compounds. The case of 2,2'-bipyridyl and its copper complex formed *in situ*. *Thermochim Acta*. 2008;467:1–10.
16. Yamanaka S, Tanaka M. Formation region and structural model of γ -zirconium phosphate. *J Inorg Nucl Chem*. 1979;41:45–8.
 17. Alberti G, Costantino U, Torracca E. Influence of thermal treatment on the rate of ion-exchange of zirconium phosphate. *J Inorg Nucl Chem*. 1966;28:225–31.
 18. Hultgren R, Desai PD, Hawkins DT, Gleiser M, Kelley KK, Wagman DD. Selected values of the thermodynamic properties of the element. Metals Park, OH: American Society for Metals; 1973.
 19. Flynn JH, Wall LA. A quick direct method for the determination of activation energy from thermogravimetric data. *J Polym Sci B*. 1966;4:323–8.
 20. Ozawa T. A new method of analyzing thermogravimetric data. *Bull Chem Soc Jpn*. 1965;38:1881–6.
 21. Gao X, Chen D, Dollimore D. The correlation between the value of α at the maximum reaction rate and the reaction mechanisms. A theoretical study. *Thermochim Acta*. 1993;223:75–82.
 22. Doyle CD. Estimating isothermal life from thermogravimetric data. *J Appl Polym Sci*. 1962;6:639–42.
 23. Kissinger HE. Reaction kinetics in differential thermal analysis. *Anal Chem*. 1957;29:1702–6.
 24. Vyazovkin S, Wight CA. Ammonium dinitramide: kinetics and mechanism of thermal decomposition. *J Phys Chem A*. 1997;101:5653–8.
 25. Coats AW, Redfern JP. Kinetic parameters from thermogravimetric data. *Nature*. 1964;201:68–9.
 26. Vyazovkin S, Wight CA. Kinetics in solids. *Ann Rev Phys Chem*. 1997;48:125–49.
 27. Vyazovkin S. A unified approach to kinetic processing of non-isothermal data. *Int J Chem Kinet*. 1996;28:95–101.
 28. Mampel KL. Zeitumsatzformeln für heterogene Reaktionen an Phasengrenzen fester Körper. 2. Die Zeitumsatzformeln für ein Pulver aus kugelförmigen Teichen. *Z Phys Chem A*. 1940;187:235–49.